Contribution to the quaternary system H 2 O–Al 3+ , Ca 2+ //O 2– , SO 4 2 – : Solid–liquid equilibria in the ternary systems Al 2 (SO 4) 3 –CaSO 4 –H 2 O and Al 2 O 3 –SO 3 –H 2 O at 25 °C

Angélique Teyssier, Jean-Michel Schmitt, Rodica Chiriac, Christelle Goutaudier

Contribution to the quaternary system H_2O–Al^{3+}, Ca^{2+} // O^{2-}, SO_4^{2-}: Solid-liquid equilibria in the ternary systems $Al_2(SO_4)_3$–$CaSO_4$–H_2O and Al_2O_3–SO_3–H_2O at 25°C

Angélique Teyssier [1,2], Jean-Michel Schmitt [1], Rodica Chiriac [2], Christelle Goutaudier [2]

[1] *AREVA, BG Mines, 1 Place Jean Millier, 92084 Paris la Défense cedex, France ;*

[2] *Université de Lyon, Université Claude Bernard Lyon 1, Laboratoire des Multimatériaux et Interfaces, UMR CNRS 5615, 69622 Villeurbanne cedex, France*

(corresponding author: angelique.teyssier@outlook.com)

Abstract: During the acid processing of aluminosilicate ores, the temporary precipitation of a white solid phase principally consisting in calcium sulfate and aluminium hydroxide and/or sulfates may be observed. This study aimed to determine the nature of the solid phases, their stability and their solubility. Understanding why precipitation occurs and being able to prevent it would help avoid the clogging that may occur during acid ore mining. Thus the solid-liquid equilibria of the two ternary systems $Al_2(SO_4)_3$–$CaSO_4$–H_2O and Al_2O_3–SO_3–H_2O were defined. The first ternary highlights very low gypsum solubility, which explains why this mineral is observed so often during acid mining. However no double Al-Ca compound, in equilibrium with a liquid phase, was found. The determination of the second system was more complex as a large number of aluminium hydroxysulfates, which could appear during the ore processing, have been reported in the literature. Most of these solid phases are poorly crystallised and not well defined as they decompose rapidly and are often metastable. The use of different techniques of characterisation (X-ray diffraction, thermogravimetry, scanning electron microscopy...) enabled the chemical composition of the solid phases to be found and also their solubility curves to be delimited. One of the aluminium hydroxysulfates decomposes rapidly when the mother solution is removed. This underlines the poor aluminium hydroxysulfate stability, which explains the difficulties in characterising them.

Keywords: solid-liquid equilibria; solubility; ore mining; aluminium hydroxysulfate characterisation; $Al_8(SO_4)_5(OH)_{14}.34H_2O$

1. Introduction

Natural ores mined to extract various metallic cations are often composed of a variety of aluminosilicates. These include feldspars (calcium, potassium or sodium aluminosilicates) and iron-magnesium aluminosilicates. During the acid processing of these ores, the temporary precipitation of solid phases may be observed. This frequently leads to over-consumption of reactants or even stops operation due to clogged industrial equipment. As a consequence, precipitates have to be removed and the cost of such a process is very high. Understanding the nature of these solid phases and how they appear would help to overcome the major challenge of avoiding precipitation and improve processing conditions.

A white precipitate is very often observed. Analyses have shown that aluminium, calcium and sulfates are the major constituents of the precipitates, as calcium sulfate and aluminium hydroxide and/or sulfate. Besides these, a large number of aluminium hydroxysulfates, which may be formed in acid mine drainage or in acid water rich in sulfate, have been reported in the literature [1-8]. These aluminium hydroxysulfates may be the potential precipitates causing clogging. However, the solid phases are often amorphous or poorly crystallized, hence complex to characterise. They are also generally absent from current thermodynamic databases so they need to be better defined. For this purpose, it is necessary to study the liquid-solid equilibria in a complex system: the isothermal and isobaric H_2O–Ca^{2+}, Al^{3+} // O^{2-}, SO_4^{2-} quaternary diagram defined on the basis of the observed precipitates as represented in Fig.1 by the basic components Al_2O_3, $Al_2(SO_4)_3$, CaO, $CaSO_4$ and H_2O. To determine this system, binaries, located on the edges of the pyramid, and ternaries, corresponding to its faces, need to be studied at 25°C and 1 atm, which are the average temperature and pressure of the operations.

Binaries and several ternaries especially those involving calcium oxide or hydroxide have already been described in the cement chemistry [9-16]. These solids are found in alkaline environments thus are generally absent in the acid processing of ores. Since the solid phases observed are calcium sulfate and aluminium hydroxysulfate, $Al_2(SO_4)_3$-$CaSO_4$-H_2O and Al_2O_3-SO_3-H_2O are the two systems considered.

1.1. Aqueous binary systems

Since temperature and pressure are fixed, determining an aqueous binary system at 25°C is similar to determining the solubility of a compound in pure water at 25°C. Al_2O_3 is not soluble in pure water at this temperature, so only the solubilities of aluminium sulfate and calcium sulfate, which are already known ($Al_2(SO_4)_3$: 27.8 w% ± 0.4 w% [1, 17-19] and $CaSO_4$: 0.208 w% ± 0.005 w% [10, 11, 15, 20]), are studied. At this temperature, in saturated solutions, solid phases exist as hydrated solids. However if it is certain that the stable solid phase for calcium sulfate at 25°C is gypsum ($CaSO_4.2H_2O$), there is an uncertainty about the number of water molecules in the stable aluminium sulfate hydrate $Al_2(SO_4)_3.nH_2O$ at this temperature: n=16 [17, 19, 21, 22], n=17 [1, 23] and n=18 [24] molecules of water were found in literature.

1.2. Aqueous ternary system $Al_2(SO_4)_3$–$CaSO_4$–H_2O

Few reliable data were found in literature about this system at 25°C. Jones [12] found two points of the solubility curve for very low aluminium sulfate concentrations, which are 0.192 w% $CaSO_4$, 0.146 w% $Al_2(SO_4)_3$ and 0.203 w% $CaSO_4$, 0.040 w% $Al_2(SO_4)_3$. These liquids are in equilibrium with gypsum. There are no data for concentrated aluminium sulfate solutions.

1.3. Aqueous ternary system Al_2O_3–SO_3–H_2O

The solid-liquid equilibria have already been represented for this system at 25°C [1, 21, 25], 60°C [26] and above 100°C [27]. Nevertheless little data are available about solid phases, especially in the more basic area for low sulfur trioxide concentrations. Bassett and Goodwin [21] and Bigham and Nordstrom [1, 28] reported a large number of stable or metastable aluminium hydroxysulfates, listed in Table 1[1], which are, in most cases, poorly crystallised. Glassy solids or gels were also observed, sometimes mixed with very small crystals. Reaching the thermodynamic equilibrium could take weeks or months, so the determination of the solid phases was not trivial. The authors also noticed the possibility of solid phases evolving after solution removal or during filtration. It was particularly difficult to determine the number of water molecules in some aluminium hydroxysulfate hydrates and the composition of the solids was often not really known. Moreover, the ICCD (International Centre for Diffraction Data) database's reference records are old, low-quality and most of them have been deleted from the database. Consequently, there are little data about the crystal structures of these solid phases.

The aims of this work were to determine the solid-liquid equilibria at 25°C in the $Al_2(SO_4)_3$–$CaSO_4$–H_2O and Al_2O_3–SO_3–H_2O ternary systems, in order to define aqueous phase compositions and to identify and characterise the solid phases. A statistical study on single-crystal X-ray diffraction led to identifying the stable aluminium sulfate hydrate at 25°C.

[1] Several solid phases, with high sulfur trioxide content, were also reported in literature [19], but are not given in Table 1.

2. Material and methods

2.1. Mixture preparation

2.1.1. Binary systems and $Al_2(SO_4)_3$–$CaSO_4$–H_2O

Aluminium sulfate octadecahydrate (Sigma-Aldrich®, ≥ 98 % purity) and calcium sulfate dihydrate (Sigma-Aldrich®, ≥ 99 %) were used to prepare mixtures. Aluminium sulfate and/or calcium sulfate were weighed in a centrifuge tube, and the exact amount of deionised water was added. A stirrer bar was added to each solution and tubes were put in a thermostated reactor where mixtures were stirred for about one week, which was long enough to reach the equilibrium state, based upon titrations conducted at one week, one month and longer, without change.

2.1.2. Ternary system Al_2O_3–SO_3–H_2O

Based on the method already described in literature [21]-[29], solutions were prepared with aluminium metal and sulfuric acid (Sigma-Aldrich®, p.a., 95.0-97.0 % purity), however no mercury or another catalyst was used. Solutions of 40 g were prepared to have enough liquid samples for chemical analyses after phase separation. The desired quantities of deionised water and sulfuric acid were weighed in a centrifuge tube. As the action of sulfuric acid on aluminium leads to dihydrogen formation, aluminium was weighed separately and added portionwise, and centrifuge tubes were opened often to avoid pressure increases and exploding tubes. When all aluminium was in solution, tubes were put in a thermostated reactor, where mixtures were stirred for at least 1 week for the acid region and up to 3 months for the more basic region, until the equilibrium state was reached. In some mixtures in the more basic region, precipitation did not occur after several months. A platinum wire was then added to induce the formation of solid phases. Stirring was then stopped and solutions were centrifuged to separate solid and liquid phases.

2.2. Liquid phase titration

To define the solubility curve, the liquid phase was determined by complexometric titration for cations and thermotitration for sulfates, and not by gravimetric methods.

2.2.1. Cation determination

Calcium and aluminium ions in solution were determined by a complexometric method. To avoid interference, aluminium was titrated first and calcium was titrated second, after aluminium complexation. Titration was done automatically using an automatic burette [Titrando® 905, Metrohm] and a photometric sensor [Optrode, Metrohm]. As the photometric sensor had eight available wavelengths (from 470 to 660 nm), it allowed selective titration of ions in solution. Detection of colour change was also more sensitive with the sensor than the human eye. *Tiamo*™ was the software used to handle data and determine end-point.

Indirect titration was used to determine aluminium ion concentration. A sample was taken and an excess of 1,2-diaminocyclohexanetetraacetic acid disodium salt solution (DCTA, Fluka, 0.1 $mol.L^{-1}$) was added to the sample and warmed for a few minutes to complex aluminium. After cooling, the mixture was buffered with hexamethylenetetramine (Sigma-Aldrich®, ≥ 99.5 % purity) around pH = 5 and a coloured indicator, xylenol orange (Sigma-Aldrich®, ACS Reagent) in KCl, was added. The solution was yellow, which is the colour of the free indicator in solution. Next, excess DCTA was titrated with zinc sulfate solution (Fluka, 0.05 $mol.L^{-1}$) at 574 nm until the solution turned red, the colour of indicator-Zn^{2+} complexes.

To determine calcium ion concentration, an excess of triethanolamine (Sigma-Aldrich®, ≥ 99 % purity) was added and the sample was warmed for a few minutes to complex aluminium ions and avoid interference or aluminium hydroxide precipitation with the pH increase. After cooling, sodium hydroxide solution was added to the mixture to reach a pH near 12 – 12.5. Murexide (Sigma-Aldrich®, ACS Reagent) in KCl was added as

coloured indicator and the solution became pink due to the formation of indicator-Ca^{2+} complexes. Finally, calcium ions were titrated with ethylenediaminetetraacetic acid disodium salt solution (EDTA, Fluka, 0.01 mol.L^{-1}) at 610 nm until the solution turned purple, which is the colour of the free indicator in solution.

Each titration was performed at least three times with good reproducibility.

2.2.2. Sulfate determination

Sulfate ions were determined by thermometric titration. Barium chloride solution was added to the mixture, leading to the precipitation of barium sulfate. Titration was done automatically using an automatic burette [859 Titrotherm, Metrohm] and a temperature sensor [Thermoprobe, Metrohm]. *Tiamo*™ was the software used to handle data and to determine end-point.

In the sample, deionised water and ethanol were added in a ratio 3:1, as experiments showed that better results were obtained with ethanol [30] since barium sulfate is nearly insoluble in water and insoluble in ethanol. In some samples, hydrochloric acid was added to prevent aluminium hydroxide precipitating due to too high a pH. Sulfate ions were then titrated with barium chloride solution at 1.0 mol.L^{-1} (Sigma-Aldrich®, ≥ 99 % purity). When the reaction took place, the temperature of the solution increased until the end-point and this change was monitored according to the volume of titrant added. After the end point the temperature was stable or decreased.

Each titration was performed at least three times with good reproducibility.

2.3. Solid phase characterisation

2.3.1. Structural characterisation by X-ray diffraction

The solid phases were determined using powder X-ray diffraction (XRD) or single-crystal X-ray diffraction, according to the nature of the solid. If solid phases were determined by powder X-ray diffraction, experimental diffractograms were compared with the ICDD database.

XRD powder analyses were recorded on a BRUKER D8 Advance diffractometer or on a Panalytical X'PertPro MRD diffractometer with a copper anticathode tube (λ (Cu Kα1) = 1.54060 Å, λ (Cu Kα2) = 1.54443 Å), in air at room temperature. Both of them have a Bragg-Brentano configuration in θ/θ (fixed sample). To prepare the sample, some solid phase was taken from the biphasic mixture and rapidly dried with a filter paper to avoid the possible decomposition or dehydration of the solid. The solid phase was then deposited on a specific holder. Time of experiment depended on the solid phase, its crystallinity and its stability after the mother solution was removed. The diffractograms which were obtained were compared to the ICDD database using the X'Pert HighScore software.

Single-crystal X-ray diffraction data were collected at room temperature on an Oxford Gemini diffractometer with a molybdenum anticathode tube (λ (Mo Kα) = 0.71073 Å) and equipped with a CCD camera. An analytical absorption correction based on the crystal shapes was applied. The structures were solved by direct methods using the SIR97 program combined with Fourier difference analyses, and refined against F ($I/\sigma(I) > 3$) by using the CRYSTALS program. All non-hydrogen atoms were anisotropically refined.

2.3.2. Determination of solid phase compositions

If the solid was amorphous or could not be identified in the database, titration of the solid was required. The dry or moist solid phase was dissolved in water with small amount of hydrochloric acid, and each element of the solid was determined as described for the liquid phase.

Some samples were also determined using energy-dispersive X-ray spectroscopy (EDS) and scanning electron microscopy (SEM) [FEI Quanta FEG 250], either to confirm XRD determination or to obtain an elementary analysis when comparison with the ICDD database led to more than one possibility.

For the more basic solid phase, titration of the solid phase was not accurate and the EDS results only gave the Al/S ratio. As a consequence thermogravimetric analyses were done using a thermogravimetric analyser [TGA/DSC 2 HT, Mettler Toledo]. The measurements were carried out in a flowing nitrogen atmosphere and a temperature range from 30 to 1200°C in a 150 µL alumina crucible with a pierced lid. The heating rate was $10°C.min^{-1}$ and the mass of the samples was about 10-11 mg. A blank analysis with empty crucibles was run before sample analyses and then the blank curve was subtracted from the sample curve. The first derivative curve (DTG) was used to evaluate the mass loss steps.

3. Results and discussion

3.1. Aqueous binary systems at 25°C under atmospheric pressure

The solubility limits and the stable solid calcium sulfate and aluminium sulfate phase were determined at 25°C and compared to data available in literature as shown in Table 2. No significant differences in the solubility limits were observed. Gypsum ($CaSO_4.2H_2O$) is the stable solid phase identified, which is in accordance with the literature at this temperature. In X-ray powder diffraction, the diffractogram obtained for aluminium sulfate solid phase was compared to the diffractograms in the ICDD database. The diffractograms of aluminium sulfate hexadecahydrate, heptadecahydrate and octadecahydrate are almost the same, so it is difficult to be certain about the hydration degree of aluminium sulfate. However, after several days, small single-crystals were observed in the saturated solution of aluminium sulfate, so a statistical study was conducted on single-crystal X-ray diffraction to determine the number of water molecules present in the stable aluminium sulfate hydrate at 25°C. To have reliable data, another saturated solution was prepared and the study was conducted on five crystals from the two solutions.

The crystals look like small plates. The formula which is found by single-crystal X-ray diffraction is $[Al(H_2O)_6]_2(SO_4)_3.3.8H_2O$. As Fig.2 presents, 15.8 molecules of water are in the stable aluminium sulfate hydrate at 25°C, with 12 of them being linked with aluminium. All refinement details are available in Table 3; those of the statistical study run on the three crystals from the first solution are given in the first column. The results from the two other crystals from the second mixture are presented in the second column. As the two refinements of the statistical occupancy recovered and the two crystal structures are identical, the molecules of aluminium sulfate hydrate have the same number of uncoordinated water molecules, taking into account the uncertainty of the refinement.

Subsequently, the stable aluminium sulfate hydrate at 25°C will be noted as $Al_2(SO_4)_3.15.8H_2O$.

3.2. $Al_2(SO_4)_3$–$CaSO_4$–H_2O

Twelve mixtures were prepared to precisely describe the solid-liquid equilibria of the $Al_2(SO_4)_3$-$CaSO_4$-H_2O system in the isotherm at 25°C. Table 4 presents the initial mixtures for the liquid phase composition and the corresponding solid phase in equilibrium. Fig.3 illustrates the experimental results for this ternary diagram. As calcium sulfate is much less soluble than aluminium sulfate, the X axis is cut in order to see the liquid region, but the conodes cannot be drawn in the diagram. This isotherm shows two biphasic regions (liquid + solid): liquid + $Al_2(SO_4)_3.15.8H_2O$ and liquid + $CaSO_4.2H_2O$ and one three-phase region (liquid + two solids) with a variance of zero: liquid L_1 + $Al_2(SO_4)_3.15.8H_2O$ + $CaSO_4.2H_2O$. The composition of the invariant liquid, which was determined precisely with very low uncertainty, is 0.051 w% $CaSO_4$; 27.75 w% $Al_2(SO_4)_3$. Fig.4 illustrates the XRD patterns confirming the triphasic region. The identification of the solid phases is simple and unambiguous.

Solid-solid equilibrium regions have not been studied in this work as only the solubility curve was needed to be determined. Moreover this ternary diagram is simple as equilibrium state was reached rapidly and there is no double aluminium-calcium compound in equilibrium with a liquid phase.

3.3. Al_2O_3–SO_3–H_2O

Table 5 presents the mixtures initially prepared, the liquid phase composition and the corresponding solid phase in equilibrium. Fig.5 depicts the experimental results for the ternary diagram Al_2O_3-SO_3-H_2O at 25°C (solid lines). Bassett and Goodwin's [21] work is plotted in dashed lines and only the main differences are drawn in this diagram.

The experimental solubility curve and the two first biphasic regions: liquid + $Al_2(SO_4)_3.15.8H_2O$ (solid A), liquid + $Al(SO_4)(OH).5H_2O$ (solid J), are almost the same as those given in the literature. Two other biphasic areas are observed: liquid + solid T and liquid + solid V. This latter region is larger than the one described by Bassett and Goodwin [21]. Contrary to identifying solid phases A and J, which was simple and unambiguous, identifying solid phases T and V was more complex as the comparison with diffractograms of the ICDD database leads to more than one record for solid T and to no record for solid V.

To be in accordance with phase-rule equilibria, two biphasic domains must be separated by a triphasic area with an invariant liquid and two solid phases; three are expected: L_1 + solid A + solid J, L_2 + solid J + solid T and L_3 + solid T + solid V.

3.3.1. Identification of solid phase T

First powder X-ray diffraction analyses, done on this solid, did not enable the solid phase to be determined. Indeed, the study highlighted the rapid decomposition of the solid phase into another after liquid removal. Consequently, peaks of two or more phases are observed in the diffractograms. Fig.6 presents the diffractograms' evolution and so the time dependence of the solid phase decomposition. The main solid phase which seems to appear during decomposition corresponds to the phase described by Sabelli and Santucci [31]: $Al_3(SO_4)_2(OH)_5.9H_2O$. However, the authors analysed this solid in the presence of gypsum ($CaSO_4.2H_2O$), so some peaks in the record do not match the experimental diffractograms. A few very small peaks in the experimental pattern do not fit with the record and could be due to the formation of aluminium hydroxide.

In the second analyses, a Mylar® film was used to stop or at least to slow down the decomposition process, so as to observe only peaks of the initial aluminium hydroxysulfate which is in equilibrium with the liquid phase. The Mylar® film presents a wide peak around 26° (2θ) in powder X-ray diffraction, as showed in Figs. 10-11. Peaks obtained for the hydrated aluminium hydroxysulfate do not match the solid phase described by Bassett and Goodwin [21]: $Al_{10}(SO_4)_6(OH)_{18}.37H_2O$. However, most of them seem to fit with the $Al_{10}(SO_4)_6(OH)_{18}.31H_2O$ solid phase, but the record of this solid has been deleted from the current ICDD database. Comparison with another diffractogram in the database shows that peaks in the solid phase $Al_8(SO_4)_5(OH)_{14}.34H_2O$ correspond to those of the experimental diffractogram. This solid phase was described by Casey et al. [32]; 7 years were required for crystals to be obtained, which could be analysed by single-crystal X-ray diffraction. Based on these data, the powder diffractogram was calculated and all peaks do match the experimental ones.

To confirm its stability in the mother solution, the solid phase of the same mixture was analysed by powder X-ray diffraction at a different time (1 to 18 months) without any change in the diffraction peaks.

Aluminium and sulfate in the solid were also titrated to verify the stoichiometry. To avoid decomposition, the solid phase was not completely dried. Instead it was dried very quickly on a filter paper to remove liquid. Results of this moist solid phase titration are available in Table 6 and are represented by triangles in Fig.7. The line linking the dots which correspond to the liquid phase, the initial mixture and the moist solid phase, converge on solid phase $Al_8(SO_4)_5(OH)_{14}.34H_2O$ and not on $Al_{10}(SO_4)_6(OH)_{18}.37H_2O$.

$Al_8(SO_4)_5(OH)_{14}.34H_2O$ is the phase in equilibrium with the liquid phase and its decomposition leads to the formation of $Al_3(SO_4)_2(OH)_5.9H_2O$ and aluminium hydroxide, as described in the equation below, which agrees with X-ray diffraction analyses.

$$2\,Al_8(SO_4)_5(OH)_{14}.34H_2O \longrightarrow 5\,Al_3(SO_4)_2(OH)_5.9H_2O + Al(OH)_3 + 23\,H_2O$$

3.3.2. Identification of solid phase V

The characterisation of this phase was even more complex, as no record corresponds to this solid. In addition, depending on the initial mixture, the solid phase was crystallised to varying degrees and X-ray diffraction peaks were not all correctly defined. At this time, structural refinements by the Rietveld method have not been possible. However, there is no difference between the wet and the dry solid phase in powder XRD, so this solid does not decompose after solution is removed.

Nevertheless, the straight line linking the liquid phase and the initial mixture converge to the solid phase $Al_{10}(SO_4)_3(OH)_{24}.xH_2O$, so different techniques were used to confirm the chemical composition of solid V.

In the first step, solid phase titration was attempt, but not all the solid dissolved even with the use of concentrated hydrochloric acid. The stoichiometry of the solid phase could not be determined.

In the second step, energy-dispersive X-ray spectroscopy and scanning electron microscopy analyses were conducted on eleven samples to determine the Al/S ration and to prove that the solid is homogenous. SEM of the compound highlights the disordered formation of nanocrystalline grains (<1µm). The EDS analyses indicate that submicron size grains have an Al/S ratio between 3.01 and 3.62 which supports the formation of a solid phase like $Al_{10}(SO_4)_3(OH)_{24}.xH_2O$.

However this technique does not give any reliable data about the amount of oxygen or hydration. Consequently, thermogravimetric analyses were planned and carried out on several solid phases from the higher pH area. Experimental conditions were chosen based on previous experiments conducted on aluminium sulfate hydrate [33, 34] and especially on basic aluminium sulfates [35, 36]. The thermogravimetric curve shown in Fig.8 looks the same as those found in literature [35, 36] and presents different mass loss steps. Between 30 to 700°C, water and hydroxyl groups are lost and above 800°C, SO_3 groups evolve. As reported before, the water and hydroxyl group losses occur in several steps and correspond to 32.6% and 10.9% mass losses respectively. Physically adsorbed water is lost first, then the molecules of water coordinated to the aluminium atoms and finally dehydroxylation. The last mass loss of 18.3% is split into two steps (16.7% + 1.6%), as it was described by Földvári [36], and matches the loss of SO_3 groups. Powder XRD analysis shows that the final product is alumina, so if the hypothesis of ten atoms of aluminium in the initial molecule is right, the mass loss of 18.3% corresponds to the loss of three SO_3 groups and thus the mass losses of 32.6% and 10.9% are equivalent to 32 water molecules. Therefore the initial stoichiometry of solid V can be written as $5Al_2O_3.3SO_3.32H_2O$ or $Al_{10}(SO_4)_3(OH)_{24}.20H_2O$.

Identifying solid phases V and T completes the description of the ternary system Al_2O_3-SO_3-H_2O at 25°C and highlights the presence of four two-phase regions: liquid + $Al_2(SO_4)_3.15.8H_2O$; liquid + $Al(SO_4)(OH).5H_2O$; liquid + $Al_8(SO_4)_5(OH)_{14}.34H_2O$ and liquid + $Al_{10}(SO_4)_6(OH)_{24}.20H_2O$. Three triphasic areas were also observed: L_1 + $Al_2(SO_4)_3.15.8H_2O$ + $Al(SO_4)(OH).5H_2O$; L_2 + $Al(SO_4)(OH).5H_2O$ + $Al_8(SO_4)_5(OH)_{14}.34H_2O$ and L_3 + $Al_8(SO_4)_5(OH)_{14}.34H_2O$ + $Al_{10}(SO_4)_6(OH)_{24}.20H_2O$. The XRD patterns shown in Figs.9-11 respectively confirm the delineation of these three regions.

The compositions of the liquid invariants are: L_1 (0.198 w SO_3; 0.086 Al_2O_3); L_2 (0.150 w SO_3; 0.072 Al_2O_3) and L_3 (0.047 w SO_3; 0.030 Al_2O_3).

4. Conclusion

In this work, the 25°C isotherm for the $Al_2(SO_4)_3$–$CaSO_4$–H_2O and Al_2O_3–SO_3–H_2O ternary systems have been defined experimentally under atmospheric pressure. The goals of this study were to determine the nature of the solid phases, their stability and solubility, since understanding solid phase precipitation can help prevent it and the clogging which occurs during acid ore mining.

The determination of the $Al_2(SO_4)_3$–$CaSO_4$–H_2O system highlights only the formation of gypsum and aluminium sulfate hydrates, so there is no Al-Ca double compound in equilibrium with a liquid phase. Defining solubility curves for the aluminium hydroxysulfates in the Al_2O_3–SO_3–H_2O ternary was more complex, as there are a large number of aluminium hydroxysulfates reported in the geological, geochemical and chemical literature. Most of these solids are not well defined, as they are amorphous or poorly crystallised, dehydrate rapidly, and are often metastable. However, the use of X-ray diffraction and other techniques led to the characterisation of the stable solid phases in the ternary systems. Some inconsistencies about these phases have been resolved, in particular the degree of hydration in some hydroxysulfates. The rapid change of some aluminium hydroxysulfates was also underlined with the decomposition of solid T when the mother solution is removed. Once again, this proves that characterising and determining the chemical composition of these phases is not simple.

In future work, to predict the appearance of these aluminium hydroxysulfates during ore processing the solubility constants will be determined by modelling the experimental results.

Acknowledgements

This work has been supported by CIFRE/ANRT doctoral grant no. 2012/0596.

References

1. Nordstrom, D. K., The effect of sulfate on aluminum concentrations in natural waters: some stability relations in the system Al2O3-SO3-H2O at 298 K. *Geochimica Et Cosmochimica Acta* **1982,** *46* (4), 681-692.
2. Myneni, S. C. B.; Traina, S. J.; Logan, T. J., Ettringite solubility and geochemistry of the Ca(OH)2–Al2(SO4)3–H2O system at 1 atm pressure and 298 K. *Chemical Geology* **1998,** *148* (1–2), 1-19.
3. Shum, M.; Lavkulich, L., Speciation and solubility relationships of Al, Cu and Fe in solutions associated with sulfuric acid leached mine waste rock. *Environmental Geology* **1999,** *38* (1), 59-68.
4. Dill, H. G., The geology of aluminium phosphates and sulphates of the alunite group minerals: a review. *Earth-Science Reviews* **2001,** *53* (1–2), 35-93.
5. Shaw, S. A.; Jim Hendry, M., Geochemical and mineralogical impacts of H2SO4 on clays between pH 5.0 and −3.0. *Applied Geochemistry* **2009,** *24* (2), 333-345.
6. Jones, A. M.; Collins, R. N.; Waite, T. D., Mineral species control of aluminum solubility in sulfate-rich acidic waters. *Geochimica Et Cosmochimica Acta* **2011,** *75* (4), 965-977.
7. Sánchez-España, J.; Yusta, I.; Diez-Ercilla, M., Schwertmannite and hydrobasaluminite: A re-evaluation of their solubility and control on the iron and aluminium concentration in acidic pit lakes. *Applied Geochemistry* **2011,** *26* (9–10), 1752-1774.
8. Prietzel, J.; Hirsch, C., Extractability and dissolution kinetics of pure and soil-added synthesized aluminium hydroxy sulphate minerals. *European Journal of Soil Science* **1998,** *49* (4), 669-681.
9. Cameron, F. K.; Bell, J. M., The system lime, gypsum water at 25°. *Journal of the American Chemical Society* **1906,** *28* (9), 1220-1222.
10. Cameron, F. K.; Breazeale, J. F., Solubility of Calcium Sulphate in Aqueous Solutions of Sulphuric Acid. *The Journal of Physical Chemistry* **1902,** *7* (8), 571-577.
11. Hulett, G. A.; Allen, L. E., The solubility of gypsum. *Journal of the American Chemical Society* **1902,** *24* (7), 667-679.
12. Jones, F. E., The quaternary system CaO-Al2O3-CaSO4-H2O at 25[degree] C. *Transactions of the Faraday Society* **1939,** *35* (0), 1484-1510.
13. Jones, F. E., The Quaternary System CaO–Al2O3–CaSO4–H2O at 25°C. Equilibria with Crystalline Al2O3–3H2O, Alumina Gel, and Solid Solution. *The Journal of Physical Chemistry* **1944,** *48* (6), 311-356.
14. Taylor, H. F. W., *Cement chemistry*. 2nd ed. ed.; T. Telford: London, 1997; p 1 vol (xviii-459 p.).
15. Wang, Y.-y.; Peng, X.-y.; Chai, L.-y.; Shu, Y.-d., Phase equilibrium of CaSO4–Ca(OH)2–H2O system. *Transactions of Nonferrous Metals Society of China* **2012,** *22* (6), 1478-1485.
16. Wells, L. S.; Clarke, W. F.; McMurdie, H. F., Study of the system CaO-Al2O3-H2O at temperatures of 21° and 90° C. *Journal of Research of the National Bureau of Standards* **1943,** *30* (5), 367-409.
17. Henry, J. L.; King, G. B., The System Aluminum Sulfate--Sulfuric Acid--Water at 60°. *Journal of the American Chemical Society* **1949,** *71* (4), 1142-1144.
18. Pascal, P.; Chrétien, A.; Frambouze, Y., *Nouveau traité de chimie minérale Tome VI Bore, aluminium, gallium, indium, thallium*. Masson: Paris, 1961; p 1 vol. (XXXIX-1039 p.).
19. Taylor, D.; Bassett, H., 850. The system Al2(SO4)3-H2SO4-H2O. *Journal of the Chemical Society (Resumed)* **1952,** (0), 4431-4442.
20. Posnjak, E., The system CaSO4-H2O. *Am. Jour. Sci.* **1938,** *5th ser., 35A*, 247-272.
21. Bassett, H.; Goodwin, T. H., 480. The basic aluminium sulphates. *Journal of the Chemical Society (Resumed)* **1949,** (0), 2239-2279.
22. Bassett, H.; Watt, W., 289. Pickeringite and the system MgSO4-Al2(SO4)3-H2O. *Journal of the Chemical Society (Resumed)* **1950,** (0), 1408-1414.
23. Ho Fang, J.; Robinson, P. D., Alunogen, Al2(H2O)(SO4)3.5H2O : Its atomic arrangement and water content. *American Mineralogist* **1976,** *61*, 311-317.
24. Kuznetsov, V. G.; Imanakunov, B., X-ray diffraction investigation of solid phases in ternary aqueous systems consisting of nickel, sodium, and aluminum sulfates at 25–65°C. *J Struct Chem* **1962,** *3* (1), 44-55.
25. Dobrev, K.; Dobreva, P., Glass formation and condensation in the alumina-sulfur trioxide-water system. *Izv. Khim.* **1983,** *16* (3), 318-28.
26. Henry, J. L.; King, G. B., Phase Rule Investigation of the System Al2O3—SO3—H2O at 60°, Basic Region. *Journal of the American Chemical Society* **1950,** *72* (3), 1282-1286.
27. Dyson, N. F.; Scott, T. R., New Phases in the System Al2O3-SO3-H2O at Temperatures above 100[deg] C. *Nature* **1965,** *205* (4969), 358-359.
28. Bigham, J. M.; Nordstrom, D. K., Iron and aluminum hydroxysulfates from acid sulfate waters. *Rev. Mineral. Geochem.* **2000,** *40* (Sulfate Minerals), 351-403.
29. Johansson, G., The Crystal Structures of [Al2(OH)2(H2O)8](SO4)2.2H2O and [Al2(OH)2(H2O)8](SeO4)2.2H2O. *Acta Chemica Scandinavica A.* **1962,** *16* (2), 403-420.
30. Williams, M. B.; Janata, J., Thermometric titration of sulphate. *Talanta* **1970,** *17* (6), 548-551.

31. Sabelli, C.; Santucci, A., Rare sulfate minerals from the Cetine mine, Tuscany, Italy. *Neues Jahrbuch für Mineralogie Monatshefte* **1987,** (4), 171-182.
32. Casey, W. H.; Olmstead, M. M.; Phillips, B. L., A New Aluminum Hydroxide Octamer, [Al8(OH)14(H2O)18](SO4)5·16H2O. *Inorganic Chemistry* **2005,** *44* (14), 4888-4890.
33. Pelovski, Y.; Pietkova, W.; Gruncharov, I.; Pacewska, B.; Pysiak, J., The thermal decomposition of aluminum sulfate in different gas phase environments. *Thermochimica Acta* **1992,** *205*, 219-224.
34. Çılgı, G.; Cetişli, H., Thermal decomposition kinetics of aluminum sulfate hydrate. *J Therm Anal Calorim* **2009,** *98* (3), 855-861.
35. Kloprogge, J. T.; Geus, J. W.; Jansen, J. B. H.; Seykens, D., Thermal stability of basic aluminum sulfate. *Thermochimica Acta* **1992,** *209*, 265-276.
36. Földvári, M., *Handbook of thermogravimetric system of minerals and its use in geological practice*. Geological Institute of Hungary (=Magyar Állami Földtani Intézet): Budapest, 2011; p 1 vol. (180 p.).

List of tables

Table 1. Aluminium sulfates and hydroxysulfates reported in the literature.

Mineral name	Formula	Stoichiometry in the Al_2O_3-SO_3-H_2O system	ICDD record
Aluminite	$Al_2(SO_4)(OH)_4.7H_2O$	$Al_2O_3.SO_3.9H_2O$	00-043-0669 (I)
Alunogen	$Al_2(SO_4)_3.17H_2O$	$Al_2O_3.3SO_3.17H_2O$	00-026-1010 (I)
	$Al_2(SO_4)_3.16H_2O$	$Al_2O_3.3SO_3.16H_2O$	00-049-1096 (O)
	$Al_2(SO_4)_3.18H_2O$	$Al_2O_3.3SO_3.18H_2O$	00-014-0559 (B-D)
Basaluminite	$Al_4(SO_4)(OH)_{10}.5H_2O$	$2Al_2O_3.SO_3.10H_2O$	00-008-0064 (I-D)
Doughtyite	$Al_4(SO_4)(OH)_{10}.7H_2O$	$2Al_2O_3.SO_3.12H_2O$	/
Felsoebanyaite	$Al_4(SO_4)(OH)_{10}.4$ or $5H_2O$	$2Al_2O_3.SO_3.10$ or $11H_2O$	00-042-0556 (I)
Hydrobasaluminite	$Al_4(SO_4)(OH)_{10}.36H_2O$	$2Al_2O_3.SO_3.41H_2O$	00-008-0076 (I)
Hydronium alunite	$(H_3O)Al_3(SO_4)_2(OH)_6$	$3Al_2O_3.4SO_3.9H_2O$	00-016-0409 (S)
Jurbanite	$Al(SO_4)(OH).5H_2O$	$Al_2O_3.2SO_3.11H_2O$	01-073-1577 (C)
Meta-aluminite	$Al_2(SO_4)(OH)_4.5H_2O$	$Al_2O_3.SO_3.7H_2O$	00-032-0027 (I)
Metaalunogen	$Al_2(SO_4)_3.14H_2O$	$Al_2O_3.3SO_3.14H_2O$	00-022-0023 (I)
Metabasaluminite	$Al_4(SO_4)(OH)_{10}$	$2Al_2O_3.SO_3.5H_2O$	00-008-0080 (B-D)
Paraluminite	$Al_4(SO_4)(OH)_{10}.10H_2O$	$2Al_2O_3.SO_3.15H_2O$	00-014-0622 (B-D)
Rostite	$Al(SO_4)(OH).5H_2O$	$Al_2O_3.2SO_3.11H_2O$	00-041-1382 (I)
Zaherite	$Al_{12}(SO_4)_5(OH)_{26}.20H_2O$	$6Al_2O_3.5SO_3.33H_2O$	00-038-0379 (I)
	$Al_2(SO_4)(OH)_4.4.78H_2O$	$Al_2O_3.SO_3.6.78H_2O$	00-011-0468 (O-D)
	$Al_2(SO_4)(OH)_4.3\ H_2O$	$Al_2O_3.SO_3.5H_2O$	00-011-0446 (O-D)
	$Al_2(SO_4)(OH)_4.2H_2O$	$Al_2O_3.SO_3.4H_2O$	00-011-0444(O-D)
	$Al_{26}(SO_4)_6(OH)_{66}.xH_2O$	$13Al_2O_3.6SO_3.xH_2O$	00-011-0462 (O-D)
	$Al_{26}(SO_4)_6(OH)_{66}.46H_2O$	$13Al_2O_3.6SO_3.79H_2O$	01-074-1414 (C)
	$Al_{10}(SO_4)_6(OH)_{18}.31H_2O$	$5Al_2O_3.6SO_3.40H_2O$	00-011-0461 (O-D)
	$Al_{10}(SO_4)_6(OH)_{18}.37H_2O$	$5Al_2O_3.6SO_3.46H_2O$	00-011-0496 (O-D)
	$Al_{22}(SO_4)_6(OH)_{54}.xH_2O$	$11Al_2O_3.6SO_3.xH_2O$	00-011-0463 (O-D)
	$Al_{10}(SO_4)_3(OH)_{24}.xH_2O$ (x=20-23)	$5Al_2O_3.3SO_3.xH_2O$ (x=32-35)	00-011-0465 (O-D)
	$Al_{14}(SO_4)_3(OH)_{36}.15H_2O$	$7Al_2O_3.3SO_3.33H_2O$	00-011-0467 (O-D)
	$Al_3(SO_4)_2(OH)_5.xH_2O$	$3Al_2O_3.4SO_3.xH_2O$	00-016-0398 (B)
	$Al_3(SO_4)_2(OH)_5.1.5H_2O$	$3Al_2O_3.4SO_3.8H_2O$	00-036-0540 (I)
	$Al_3(SO_4)_2(OH)_5.9H_2O$	$3Al_2O_3.4SO_3.23H_2O$	00-040-0499 (O)
	$Al_8(SO_4)_5(OH)_{14}.34H_2O$	$4Al_2O_3.5SO_3.41H_2O$	01-073-3546 (C)

I : Indexed O : Doubtful B : Blank S : Star C : Calculated D : Deleted

Table 2. Solubility limit in the binary systems $Al_2(SO_4)_3$–H_2O and $CaSO_4$–H_2O at 25°C (expressed in percent by weight).

	Literature		This work	
	Solubility limit	Solid phase	Solubility limit	Solid phase
$CaSO_4$ – H_2O	0.207% [1]	$CaSO_4.2H_2O$	0.208%	$CaSO_4.2H_2O$
	0.208% [2, 3]	$CaSO_4.2H_2O$		
	0.213% [4]	$CaSO_4.2H_2O$		
$Al_2(SO_4)_3$– H_2O	27.7% [5]	$Al_2(SO_4)_3.16H_2O$	27.76% - 27.85%	$Al_2(SO_4)_3.15.8H_2O$
	27.8% [6, 7]	$Al_2(SO_4)_3.17H_2O$		
	28.2% [8]	$Al_2(SO_4)_3.16H_2O$		

1. Posnjak, E., The system CaSO4-H2O. *Am. Jour. Sci.* **1938,** *5th ser., 35A*, 247-272.
2. Hulett, G. A.; Allen, L. E., The solubility of gypsum. *Journal of the American Chemical Society* **1902,** *24* (7), 667-679.
3. Wang, Y.-y.; Peng, X.-y.; Chai, L.-y.; Shu, Y.-d., Phase equilibrium of CaSO4–Ca(OH)2–H2O system. *Transactions of Nonferrous Metals Society of China* **2012,** *22* (6), 1478-1485.
4. Cameron, F. K.; Breazeale, J. F., Solubility of Calcium Sulphate in Aqueous Solutions of Sulphuric Acid. *The Journal of Physical Chemistry* **1902,** *7* (8), 571-577.
5. Taylor, D.; Bassett, H., 850. The system Al2(SO4)3-H2SO4-H2O. *Journal of the Chemical Society (Resumed)* **1952,** (0), 4431-4442.
6. Nordstrom, D. K., The effect of sulfate on aluminum concentrations in natural waters: some stability relations in the system Al2O3-SO3-H2O at 298 K. *Geochimica Et Cosmochimica Acta* **1982,** *46* (4), 681-692.
7. Pascal, P.; Chrétien, A.; Frambouze, Y., *Nouveau traité de chimie minérale Tome VI Bore, aluminium, gallium, indium, thallium*. Masson: Paris, 1961; p 1 vol. (XXXIX-1039 p.).
8. Henry, J. L.; King, G. B., The System Aluminum Sulfate--Sulfuric Acid--Water at 60°. *Journal of the American Chemical Society* **1949,** *71* (4), 1142-1144.

Table 3. Single-crystal X-ray diffraction refinement details for complexes 1-5 and ligand L^2.

	1LS-Al	**2LS-Al**
Empirical formula	$H_{31.43}Al_2O_{27.72}S_3$	$H_{31.46}Al_2O_{27.73}S_3$
Chemical formula	$[Al(H_2O)_6]_2(SO_4)_3.3.82(\pm0.08)\ H_2O$	$[Al(H_2O)_6]_2(SO_4)_3.3.73(\pm0.09)\ H_2O$
Molecular weight ($g.mol^{-1}$)	625.3	625.5
Crystal system	triclinic	triclinic
Space group	P-1	P-1
a (Å)	6.0519(6)	6.0519(3)
b (Å)	7.4178(6)	7.4180(5)
c (Å)	26.949(2)	26.938(1)
α (deg.)	91.803(6)	88.082(5)
β (deg.)	90.030(7)	90.029(4)
γ (deg.)	97.657(7)	82.413(5)
V ($Å^3$)	1198.4(2)	1198.1(1)
Z	2	2
T (K)	293	293
Number of independent reflexions	4894	5435
$\mathbf{R_{int}}$	0.037	0.040
R	0.0720	0.0954
$\mathbf{R_w}$	0.0777	0.0832
S	1.04	1.04
Number of used reflexions	3324	4209
Number of refined parameters	311	312

Table 4. Solid-liquid equilibrium data in the ternary system $Al_2(SO_4)_3$–$CaSO_4$–H_2O at 25°C.

	Initial mixture composition (%w)		Liquid phase composition (%w)		Solid phase in equilibrium
	$CaSO_4$	$Al_2(SO_4)_3$	$CaSO_4$	$Al_2(SO_4)_3$	
	0.000	29.71	0.000	27.80	$Al_2(SO_4)_3.15.8H_2O$
	0.019	29.02	0.023	27.78	$Al_2(SO_4)_3.15.8H_2O$
	0.034	28.40	0.040	27.71	$Al_2(SO_4)_3.15.8H_2O$
L_1	0.180	28.00	0.051	27.75	$Al_2(SO_4)_3.15.8H_2O + CaSO_4.2H_2O$
	0.201	25.02	0.074	24.97	$CaSO_4.2H_2O$
	0.206	23.02	0.088	22.98	$CaSO_4.2H_2O$
	0.250	20.03	0.112	19.94	$CaSO_4.2H_2O$
	0.635	16.00	0.144	16.14	$CaSO_4.2H_2O$
	1.003	10.02	0.173	10.13	$CaSO_4.2H_2O$
	0.252	10.02	0.171	10.09	$CaSO_4.2H_2O$
	0.998	5.02	0.185	5.10	$CaSO_4.2H_2O$
	0.490	0.00	0.208	0.00	$CaSO_4.2H_2O$

The standard uncertainties u are $u(w_{Ca}) = 0.002\%$, $u(w_{Al}) = 0.05\%$

Table 5. Solid-liquid equilibrium data in the ternary system Al_2O_3–SO_3–H_2O at 25°C.

	Initial mixture composition (w)		Liquid phase composition (w)		Solid phase in equilibrium
	SO_3	Al_2O_3	SO_3	Al_2O_3	
	0.343	0.039	0.339	0.015	$Al_2(SO_4)_3.15.8H_2O$
	0.275	0.060	0.257	0.041	$Al_2(SO_4)_3.15.8H_2O$
L_1	0.247	0.114	0.198	0.086	$Al_2(SO_4)_3.15.8H_2O + Al(SO_4)(OH).5H_2O$
	0.205	0.100	0.181	0.080	$Al(SO_4)(OH).5H_2O$
	0.200	0.100	0.166	0.075	$Al(SO_4)(OH).5H_2O$
	0.189	0.100	0.157	0.072	$Al(SO_4)(OH).5H_2O$
L_2	0.190	0.110	0.150	0.072	$Al(SO_4)(OH).5H_2O + Al_8(SO_4)_5(OH)_{14}.34H_2O$
	0.148	0.090	0.134	0.065	$Al_8(SO_4)_5(OH)_{14}.34H_2O$
	0.143	0.095	0.113	0.057	$Al_8(SO_4)_5(OH)_{14}.34H_2O$
	0.107	0.068	0.089	0.046	$Al_8(SO_4)_5(OH)_{14}.34H_2O$
	0.090	0.060	0.073	0.037	$Al_8(SO_4)_5(OH)_{14}.34H_2O$
	0.070	0.050	0.051	0.030	$Al_8(SO_4)_5(OH)_{14}.34H_2O$
	0.101	0.091	0.049	0.029	$Al_8(SO_4)_5(OH)_{14}.34H_2O$
L_3	0.060	0.055	0.047	0.030	$Al_8(SO_4)_5(OH)_{14}.34H_2O + Al_{10}(SO_4)_3(OH)_{24}.20H_2O$
	0.048	0.045	0.039	0.023	$Al_{10}(SO_4)_3(OH)_{24}.20H_2O$
	0.040	0.040	0.029	0.016	$Al_{10}(SO_4)_3(OH)_{24}.20H_2O$
	0.030	0.030	0.021	0.011	$Al_{10}(SO_4)_3(OH)_{24}.20H_2O$
	0.015	0.025	0.004	0.002	$Al_{10}(SO_4)_3(OH)_{24}.20H_2O$

The standard uncertainties u are u(w)=0.001

Table 6. Mixtures in the two-phase region: liquid–$Al_8(SO_4)_5(OH)_{14}.34H_2O$.

Initial mixture composition (w)		Liquid phase composition (w)		Moist solid phase (w)		Solid phase in equilibrium
SO_3	Al_2O_3	SO_3	Al_2O_3	SO_3	Al_2O_3	
0.143	0.095	0.113	0.057	0.201	0.181	$Al_8(SO_4)_5(OH)_{14}.34H_2O$
0.107	0.068	0.089	0.046	0.206	0.199	$Al_8(SO_4)_5(OH)_{14}.34H_2O$
0.070	0.050	0.051	0.030	0.187	0.181	$Al_8(SO_4)_5(OH)_{14}.34H_2O$

The standard uncertainties u are u(w)=0.001

List of figures

Fig. 1 Square-based pyramid representing the quaternary system H_2O-Al^{3+}, Ca^{2+} // O^{2-}, SO_4^{2-} at isothermal and isobaric conditions.

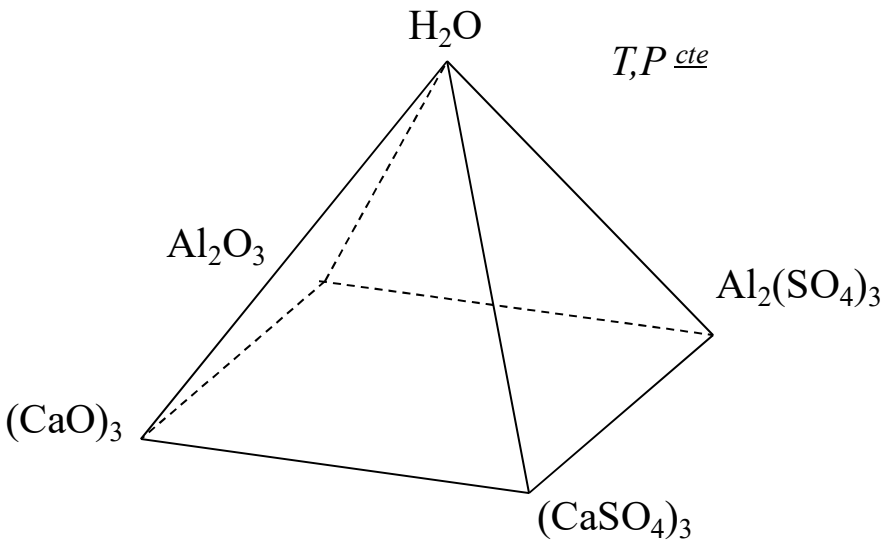

Fig. 2 XRD structure of the stable aluminium sulfate hydrate at 25°C.

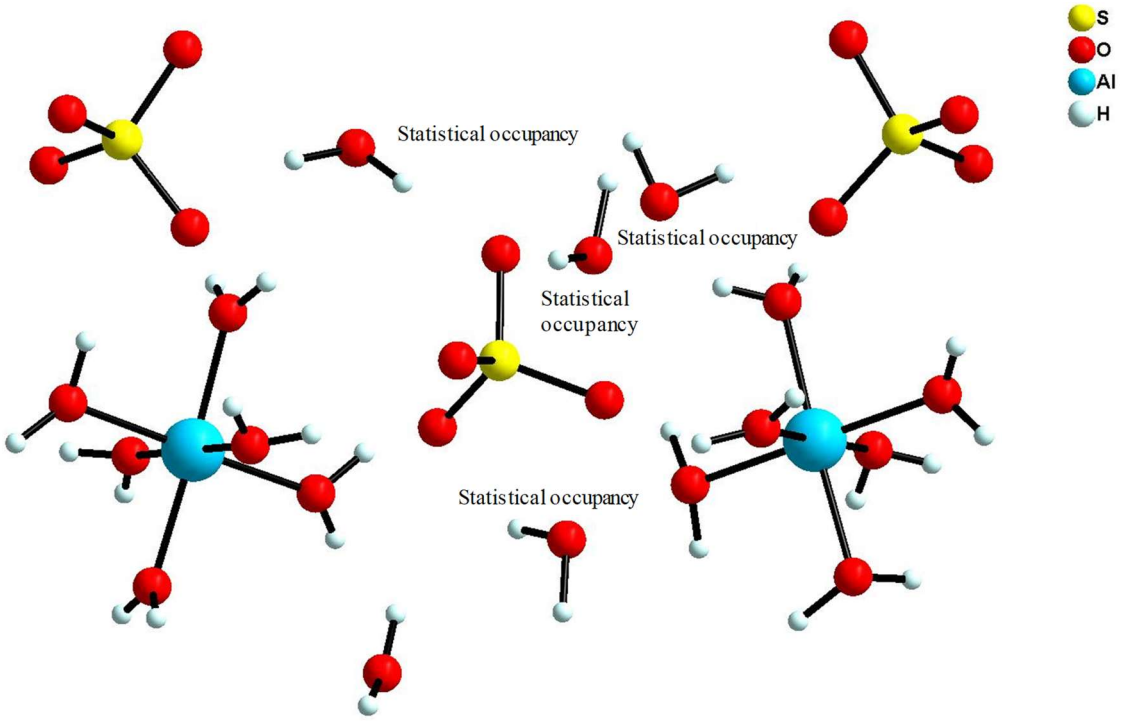

Fig. 3 Ternary system $Al_2(SO_4)_3$–$CaSO_4$–H_2O at 25°C and 1 atm.

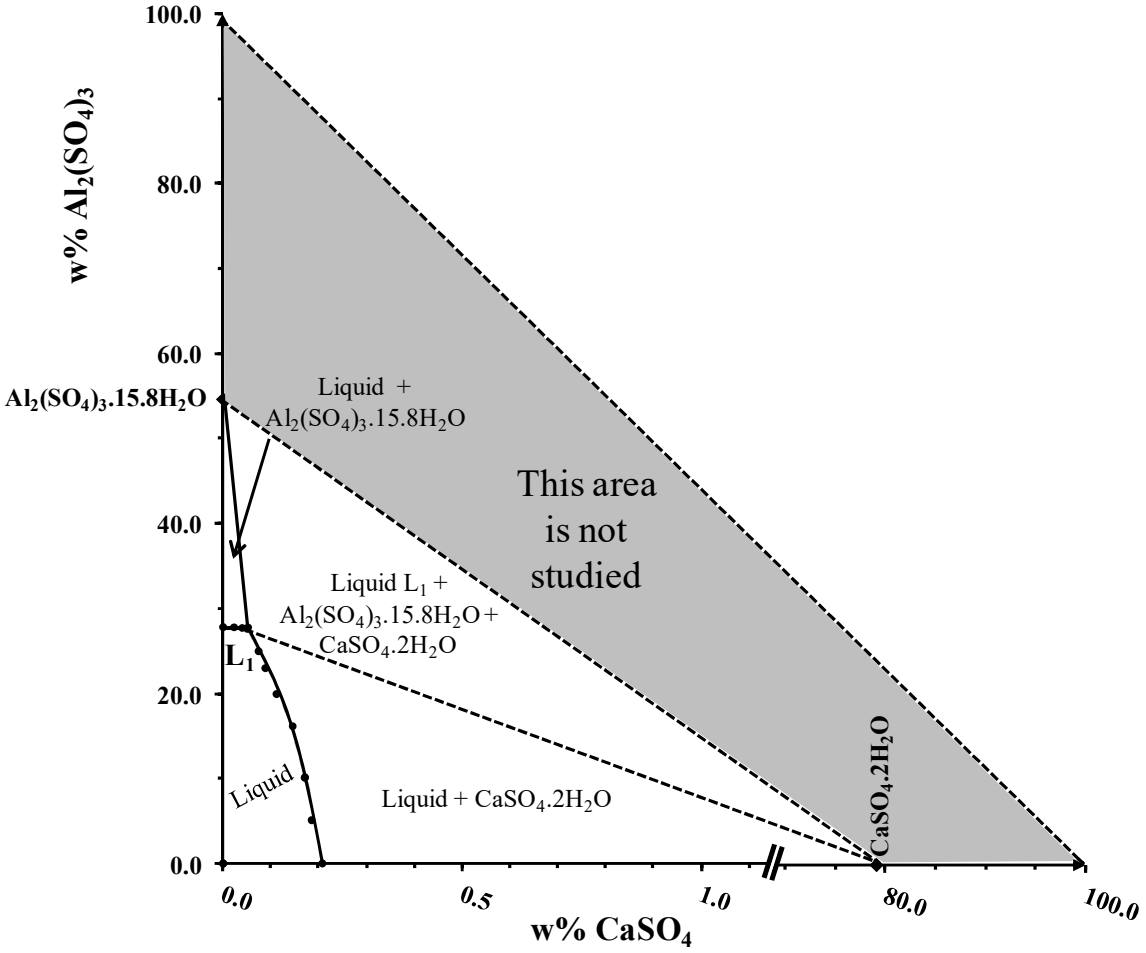

Fig. 4 XRD pattern of powder solid phase, triphasic region L_1 + $Al_2(SO_4)_3.15.8H_2O$ + $CaSO_4.2H_2O$, at 25°C.

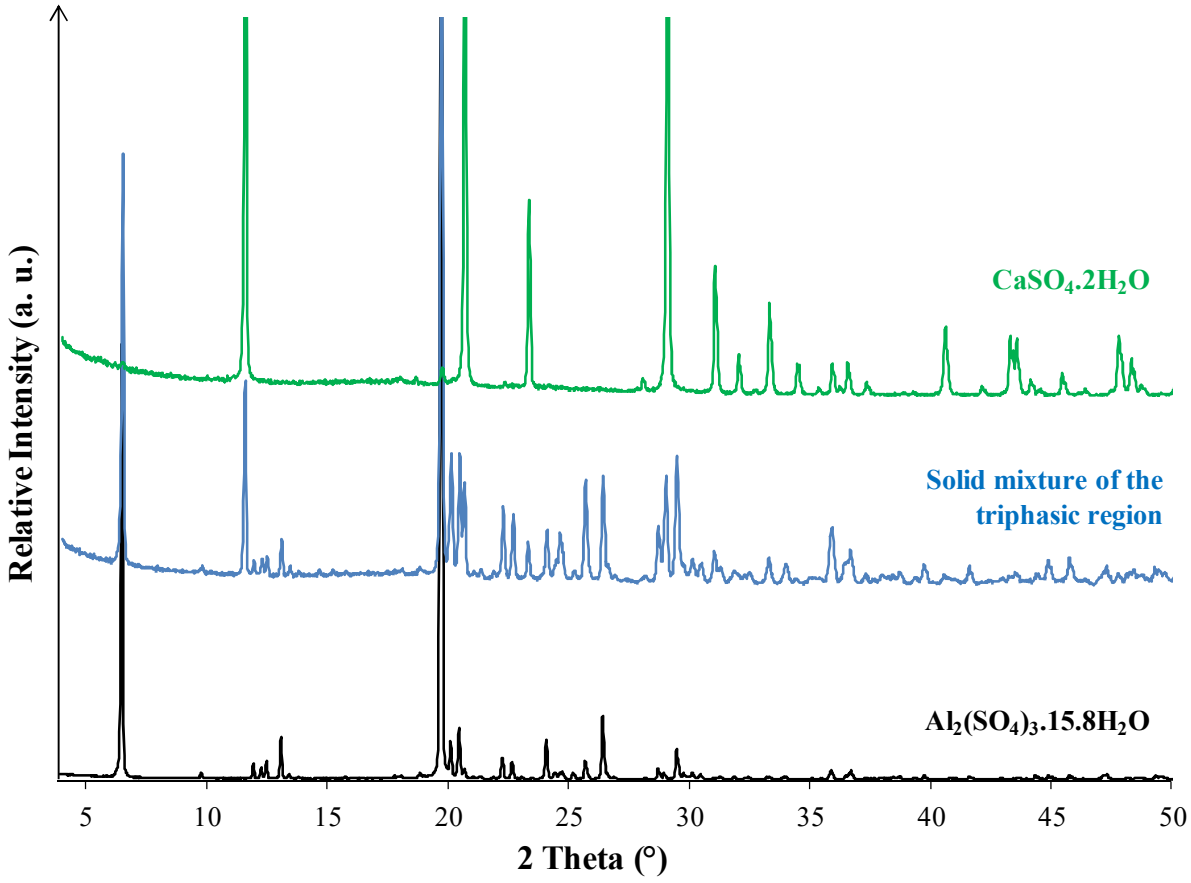

Fig. 5 Ternary system Al_2O_3–SO_3–H_2O at 25°C and 1 atm.

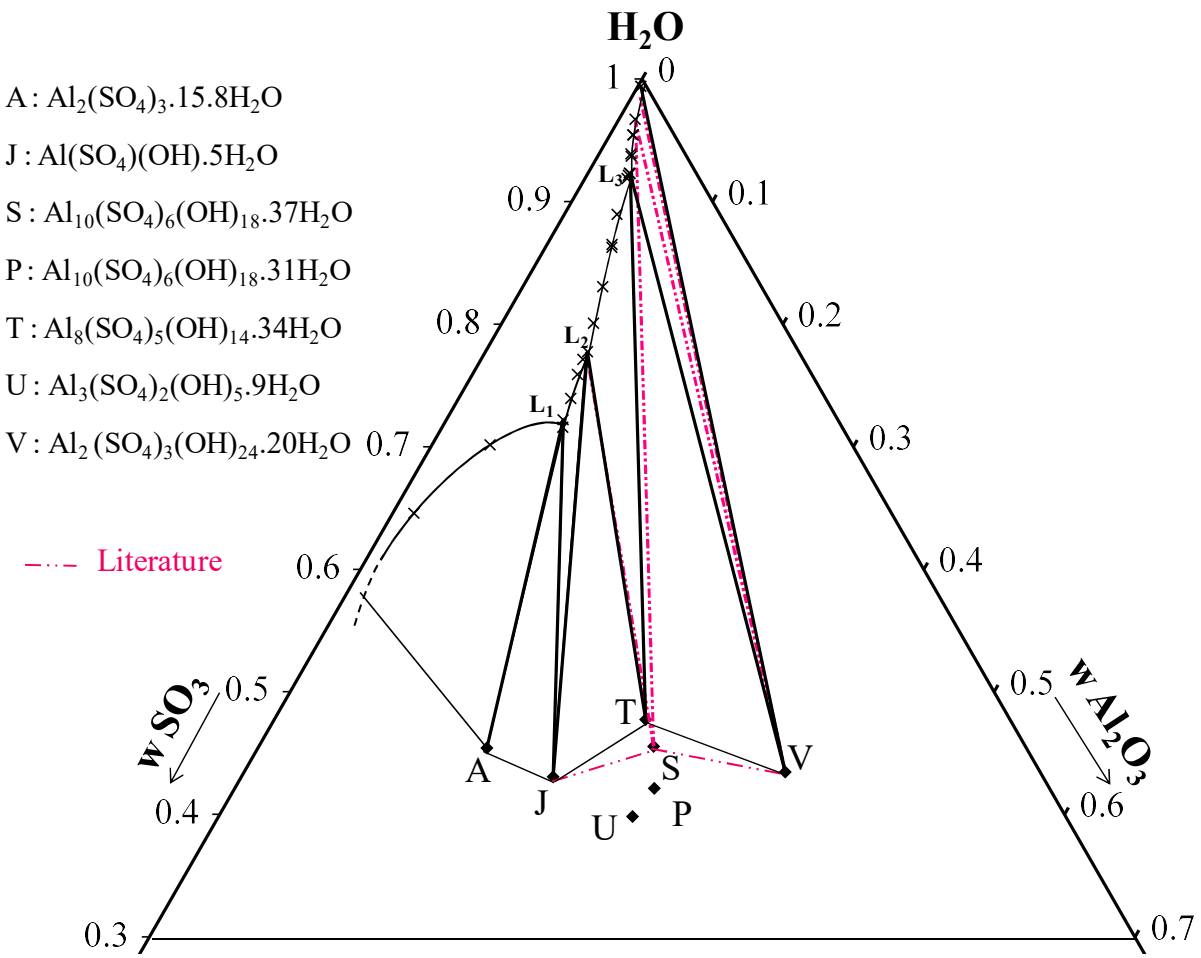

Fig. 6 Solid phase evolution of $Al_8(SO_4)_5(OH)_{14}.34H_2O$ after the solution removal. The brown XRD diffractogram is the first one, the solid phase was moist. The green one is the last one, when the solid phase was completely dry. Stars indicate the main changes.

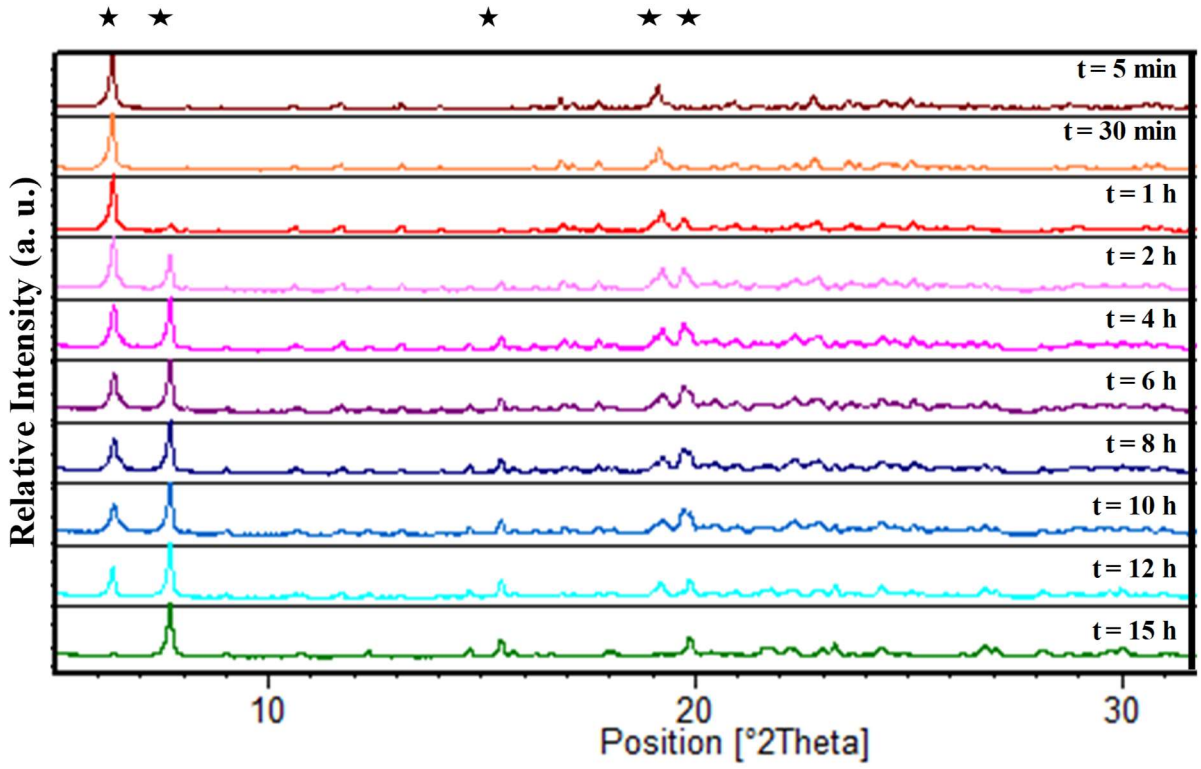

Fig. 7 Moist solid phase titration in the two-phase domain: liquid + $Al_8(SO_4)_5(OH)_{14}.34H_2O$. (Cross: liquid phase; open diamond: initial mixture; filled triangle: moist solid phase).

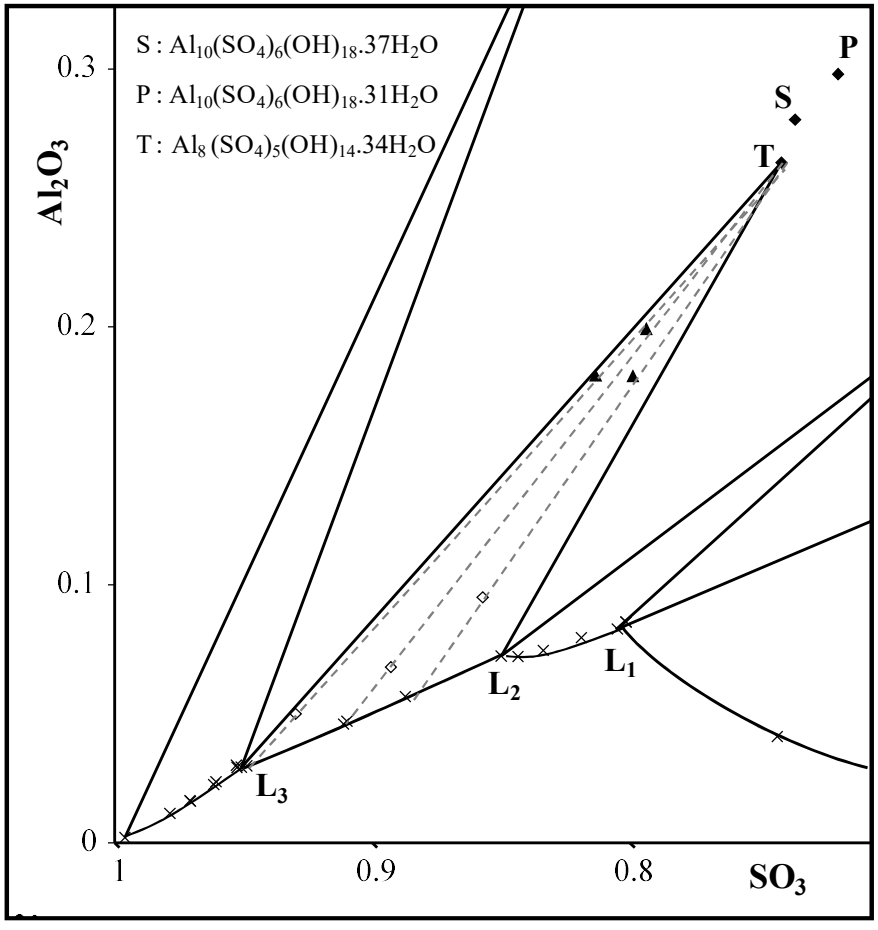

Fig. 8 Thermogravimetric curve (in solid line) and 1^{e} derivative of the thermogravimetric curve (in dashed line) of the solid phase $Al_{10}(SO_4)_3(OH)_{24}.20H_2O$.

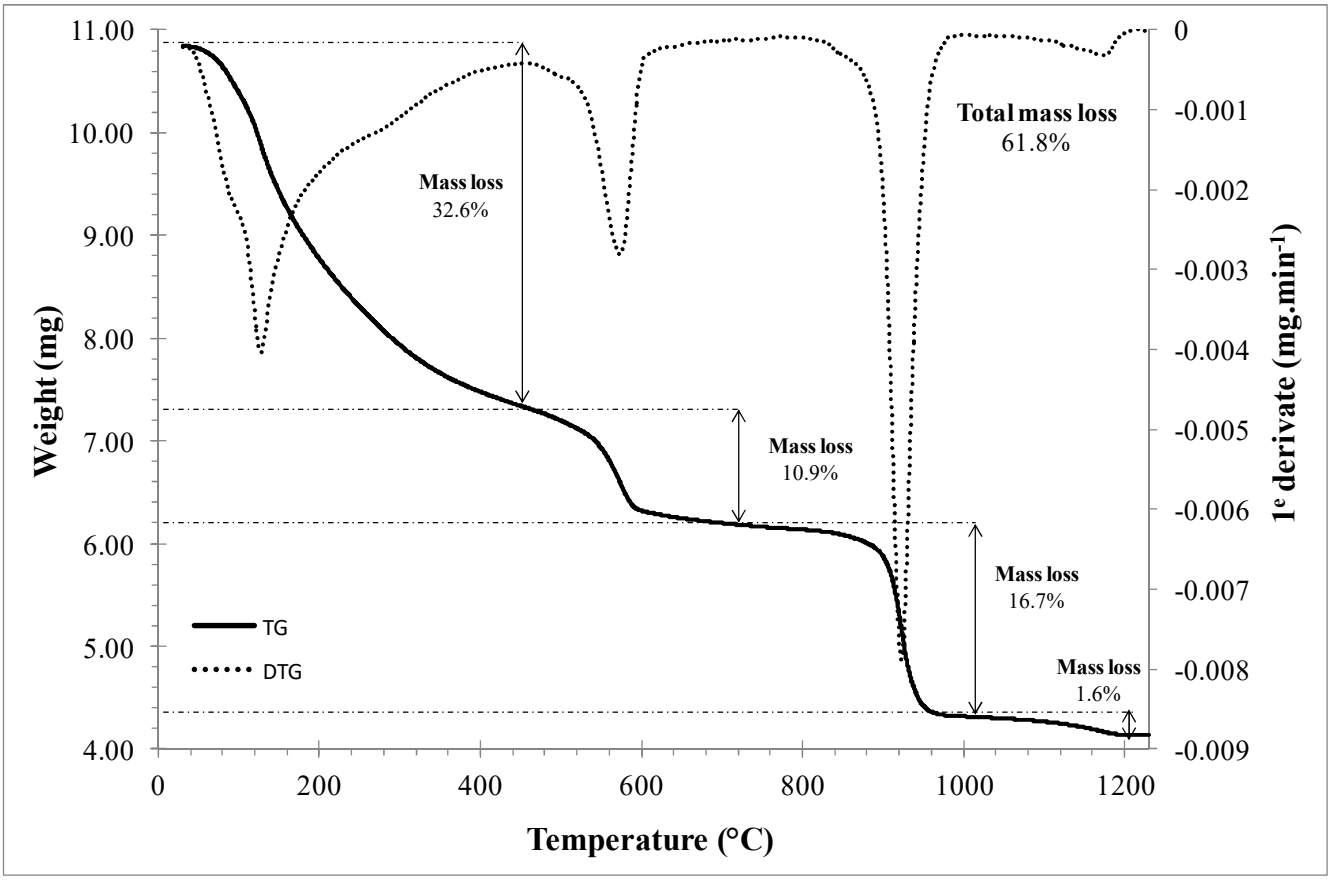

Fig. 9 XRD patterns of powder solid phase, triphasic region L_1 + $Al_2(SO_4)_3.15.8H_2O$ + $Al(SO_4)(OH).5H_2O$, at 25°C.

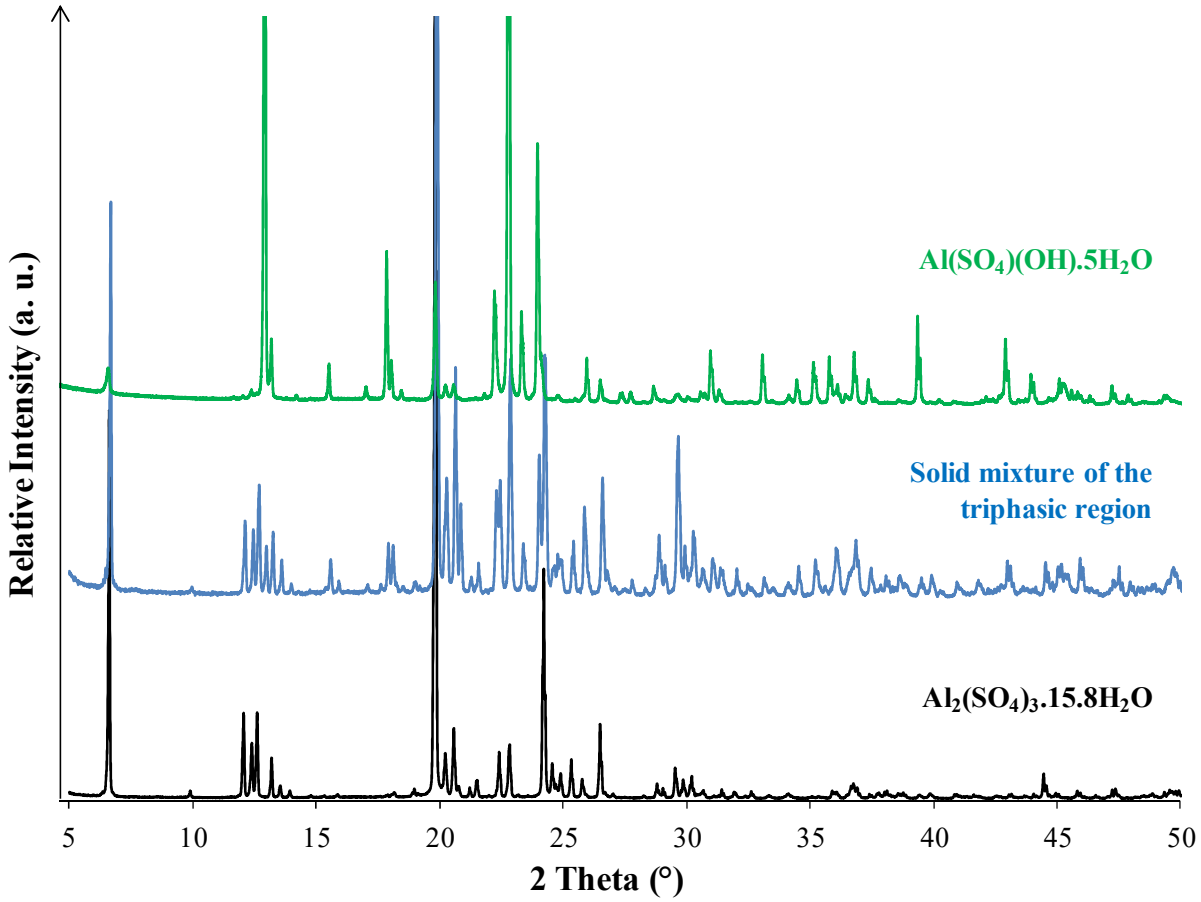

Fig. 10 XRD patterns of powder solid phase, triphasic region L_2 + $Al(SO_4)(OH).5H_2O$ + $Al_8(SO_4)_5(OH)_{14}.34H_2O$, at 25°C.

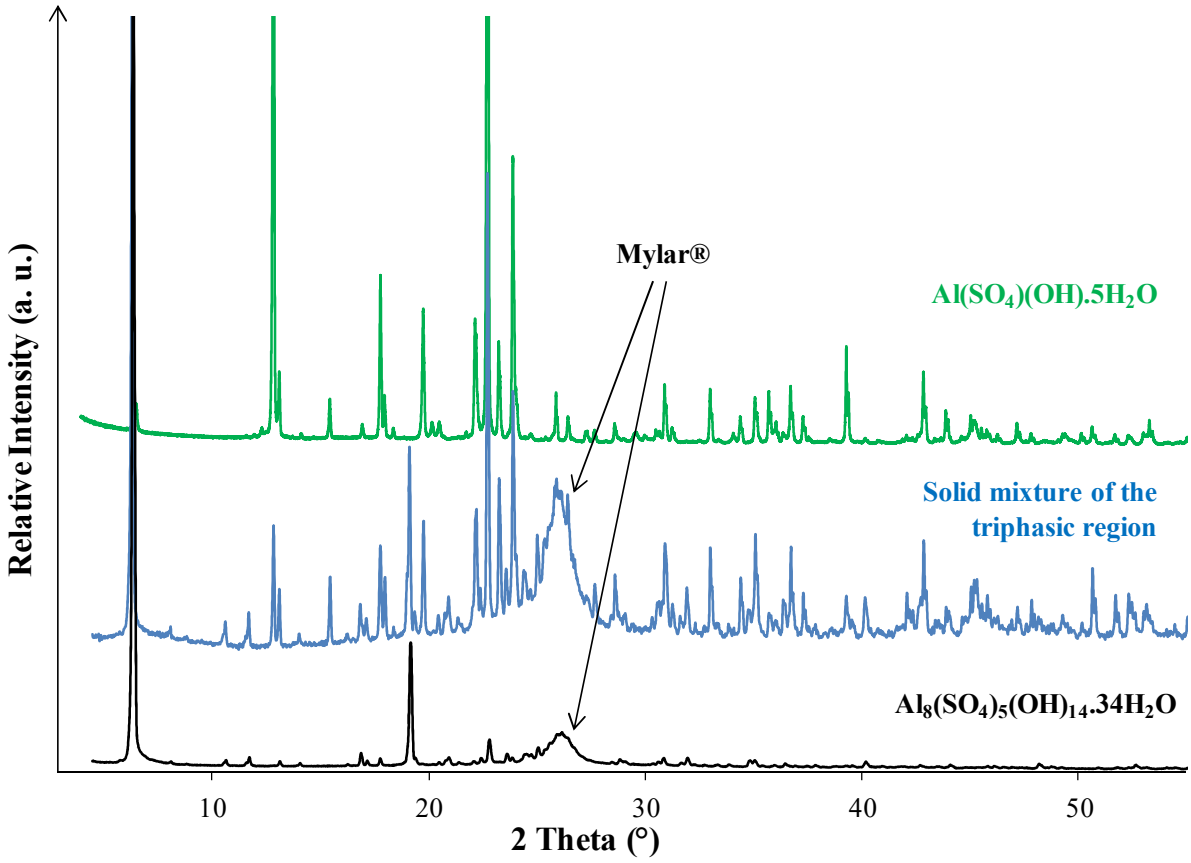

Fig. 11 XRD patterns of powder solid phase, triphasic region L_3 + $Al_8(SO_4)_5(OH)_{14}.34H_2O$ + $Al_{10}(SO_4)_3(OH)_{24}.20H_2O$, at 25°C.